

A “BOTTOM-UP” APPROACH TO ESTIMATE TAXON-SPECIFIC PRIMARY
PRODUCTION RATES ON CORAL REEFS

by

DANIEL PATRICK OWEN

(Under the Direction of Brian M. Hopkinson)

ABSTRACT

This thesis uses a “bottom-up” approach to estimate the contribution of different types of primary producers to total primary production of a coral reef. Photographic 3-D mapping was employed to build high resolution 3-D image reconstructions of the benthic ecosystem. Primary producers and their surface area were determined in the 3-D reconstruction using machine learning tools. Chamber measurements of photosynthetic rates of the major sessile components of the reef benthic community were obtained as a function of irradiance. The metabolic rates of reef community members were combined with their surface areas (obtained from the 3-D benthic maps) and a daylight irradiance model to estimate the total reef metabolism and partition total reef productivity among community members. Coral sites were estimated to have gross primary production rates ranging from 142-235 $\mu\text{mol O}_2/\text{m}^2/\text{day}$. Individual taxa contribution to total productivity was found to be related to taxa 3-D benthic cover contribution.

INDEX WORDS: primary production, ecosystem productivity, coral reef, Florida Keys, metabolic rates, productivity partitioning, productivity model, 3-D modelling.

A “BOTTOM-UP” APPROACH TO ESTIMATE TAXON-SPECIFIC PRIMARY
PRODUCTION RATES ON CORAL REEFS

by

DANIEL PATRICK OWEN
B.S., FLORIDA STATE UNIVERSITY, 2015

A Thesis Submitted to the Graduate Faculty of The University of Georgia in Partial Fulfillment
of the Requirements for the Degree

MASTERS OF SCIENCE

ATHENS, GEORGIA

2019

© 2019

DANIEL PATRICK OWEN

All Rights Reserved

A "BOTTOM-UP" APPROACH TO ESTIMATE TAXON SPECIFIC PRIMARY
PRODUCTION RATES ON CORAL REEFS

by

DANIEL PATRICK OWEN

Major Professor: Brian M. Hopkinson
Committee: William K. Fitt
James W. Porter

Electronic Version Approved:

Suzanne Barbour
Dean of the Graduate School
The University of Georgia
May 2019

DEDICATION

This work is dedicated to my father, Kevin Owen, who has always supported and helped shape my love for science and interest in the marine environment. As well, this work is dedicated to all of the mentors, scientists, friends, and peers I have met during my time at University of Georgia, Florida State University, Athens, Key Largo, Tampa, and Tallahassee. They have all motivated me, supported me, helped me stay positive, and kept me working my hardest during my time as an undergraduate and graduate student.

ACKNOWLEDGEMENTS

I would like to thank the Alfred P. Sloan Foundation for funding this work. I would also like to acknowledge Dr. Dustin Kemp and his laboratory, as well as Dr. Matthew Long whose help was vital in collecting samples in the Florida Keys. I would like to thank my committee members Dr. Brian Hopkinson, Dr. William K. Fitt, and Dr. James Porter for giving me the opportunity to experience and work in the amazing ecosystems detailed in this thesis as well as for all the patience and support they have provided on this project. All reef samples were collected in the Florida Keys National Marine Sanctuary under NOAA collecting permit #FKNMS-2016-082.

TABLE OF CONTENTS

| | Page |
|------------------------|------|
| ACKNOWLEDGEMENTS | v |
| INTRODUCTION | 1 |
| METHODS..... | 5 |
| RESULTS..... | 13 |
| DISCUSSION | 31 |
| REFERENCES | 37 |

INTRODUCTION

Coral reefs exhibit spectacular organismal diversity and have significant ecological, aesthetic and commercial value, especially in relation to fisheries and tourism (Hughes 1994). Coral reefs are also some of the most productive ecosystems on earth with clear, warm, shallow waters promoting the proliferation of numerous aquatic primary producers. The dominant primary producers on a coral reef include zooxanthellae (symbiotic photosynthetic dinoflagellates) found in hard and soft corals, and a diverse array of benthic macro- and micro-algae. Hard corals are the principal framework builders on coral reefs and are therefore the main contributor to the high level of surface habitat complexity within a reef ecosystem (Sweatman et al. 2011). The complex three-dimensional structure of coral reefs combined with the high levels of productivity found within the system support a multitude of higher trophic organisms and provides ecosystems services that support more than 275 million people world-wide (Burke et al. 2011).

Understanding how the production in a coral reef ecosystem is partitioned among community members allows insight into taxa-specific production patterns, community structure, energy flow and elemental cycling on a reef. Around half of the carbon assimilated by symbiotic zooxanthellae is exuded into the surrounding seawater by the coral host (Davies 1984). Of this exuded mucus, 60-80% immediately dissolves in the seawater and is made available as a food source for planktonic bacteria. This mucus feeds into the local microbial pelagic loop and the carbon originally fixed by hard and soft coral zooxanthellae is tightly recycled within the ecosystem (Wild et al. 2004). Compared to the production by coral symbionts, macroalgae and

turf algae are quickly grazed when herbivores are present on the reef. Macro-algal primary production therefore more directly supports higher trophic level reef organisms (Carpenter 1986).

The structure and health of coral reefs worldwide are increasingly and negatively impacted by natural and anthropogenic stressors. Coral reefs affected by decades of losses in reef herbivores due to overfishing and disease, excess of inputs of sediment and nutrients, thermally induced coral bleaching, damage from hurricanes, etc. are exhibiting community phase shifts from coral to algae dominated cover (Sweatman et al. 2011). Coral reefs in some areas have documented hard coral cover decreases from 50% cover to 5% cover in a matter of years, with little signs of recovery for decades after (Hughes 1994, Gardner et al. 2003, Graham et al. 2011). Further, in areas where the local herbivores are severely impacted, increases in macroalgae cover can produce massive amounts of labile organic matter that may increase the growth and activity of microbes that are pathogenic to corals. This may lead to a positive feedback loop for algal cover domination during recently observed phase shifts from coral to algal cover on reefs (Smith et al. 2006). In some coral reef systems, these negative stressors have severely impacted the ecosystem processes and potentially the dynamics of the ecosystem productivity. Being able to accurately partition production among reef community members will help us understand how reef community production is being affected by negative stressors, and in turn offers insight into the direction reefs may go in the future.

Scientists have been developing ways to measure coral reef ecosystem productivity for over half a century (e.g. Odum and Odum 1955 for some of the earliest work). Recent advances in ecosystem production measurements include utilizing Eddy Covariance methods to measure ecosystem metabolism in specific reef areas (Long et al. 2013). Eddy Covariance methods

provide accurate, high frequency measurements of ecosystem level reef productivity. However, “top-down” (that is, whole ecosystem) and geochemical methods of measuring productivity are unable to distinguish which organisms are responsible for metabolism measured within the environment and cannot partition productivity among reef community members. The goal of this project is to combine 3-D surface area measurements of reef transects, chamber metabolism measurements of dominant primary producers, and light modelling onto 3-D reconstructions of reefs, to produce a “bottom-up” estimate of coral reef ecosystem productivity.

The “bottom-up” (that is, additive of each of the parts) approach allows us to estimate the total primary production rates on a reef site, as well as the contribution of different types of primary producers to total primary production in the coral reefs (illustrated in Figure 1). This method relies on scaling up taxon-specific rates of production in proportion to the abundance of those taxa in the environments. First, metabolic production rates (P) of abundant autotrophic taxa are measured within chambers at increasing levels of irradiance (E). Then these productivity rates are normalized to the sample size and then scaled up to the surface area distribution on a 3-D reconstruction of a reef site. Next, the amount of light (E) striking each surface on the 3-D reef reconstruction is modeled over the course of the sunlight hours (t) of a day as a realistic function of depth. Finally, the light striking each reef surface, combined with the measured chamber productivity allows us to estimate the site-specific productivity over the course of a day and partition it among reef community members.

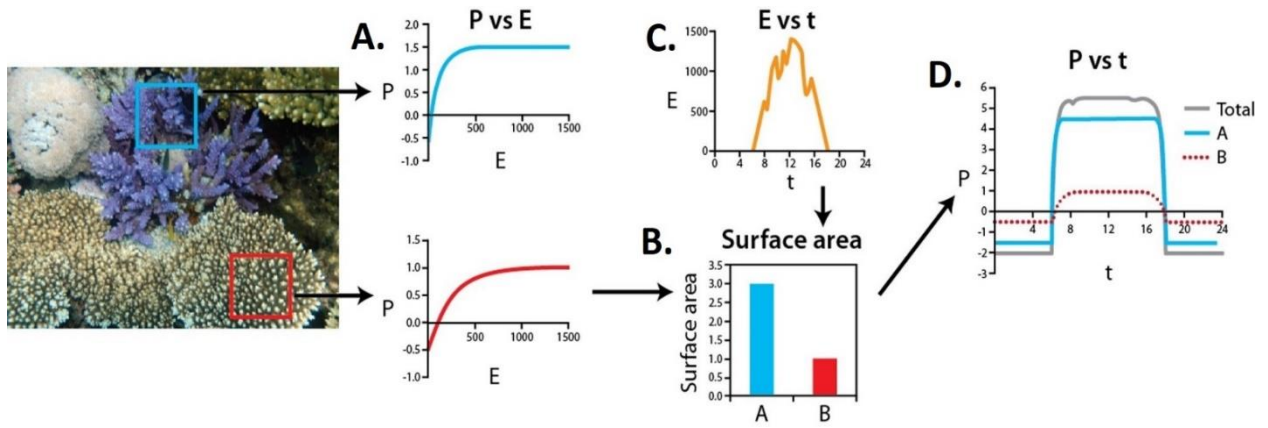


Figure 1. Outline of “bottom-up” approach to estimate taxon-specific primary production rates on coral reefs.

METHODS

Specimen Collection and Handling

Specimens were collected within Little Grecian Reef in the Northern Florida Keys (approximately N 25°06'21.6", W 80°18'25.2") under NOAA coral collecting permits issued to Dr. William K. Fitt. Sampling occurred during Winter seasons (December 2016 and December 2017) and Summer seasons (June-July 2016, 2017, and 2018). Specimens of the dominant autotrophic taxa present at each reef site were taken during sampling. Specimens taken for metabolic study included the hard corals *Orbicella annularis*, *Orbicella faveolata*, and *Porites astreoides*, and *Acropora palmata*, soft corals within the genus *Antilloporgia*, *Gorgonia ventalina*, and genus *Plexaurella* (sea rods), the algal groups *Dictyota spp.*, *Styopodium spp.*, *Halimeda spp.*, and *Galaxaura spp.*, as well as chunks of rubble with encrusting coralline algae and turf algae. Hard corals were collected by breaking off small fragments with a chisel and hammer from live coral colonies. Each hard coral was taken from a separate coral colony to reduce pseudo-replication during metabolic measurements. Macroalgae and soft corals were collected either by hand or by snipping them off the substrate with gardening shears. The point of attachment was maintained on the algae and soft coral specimens whenever possible to decrease stress on the organism. Rubble chunks were generally comprised of the dead remnants of branching and bouldering corals and were collected as whole pieces.

Specimens were immediately placed in seawater-filled Ziploc bags after removal and were transported back to laboratory in seawater filled insulated coolers. Once at shore, specimens were labelled and placed in a recirculating holding tank (Figure 2). The recirculating

tank was filled with seawater collected from the reef sampling site and featured a mechanical and UV filter, a water chiller, and water heaters. The temperature, salinity, and water level of the recirculating tank were monitored throughout the metabolic measurement in order to keep the holding tank as close to the sampling environmental conditions as possible. A mesh screen was placed over the tank during high light hours. Before being placed in the holding tanks, *Plexaurella* specimen flesh was trimmed down to the axial rod for fastening purposes. *Antilloorgia*, *Plexaurella*, and *Acropora palmata* were suspended away from the sides and the base of holding chambers to reduce stress and abrasion on the specimen. The freshly exposed bases of the hard coral chunks were covered with plasticine clay in order ensure the metabolic signal measured from the coral was only coming from the coral tissue and not cryptic species living within the coral. Coral specimens were allowed to rest for at least 24 hours in the holding tank of filtered seawater before productivity measurements were taken.



Figure 2. Specimen holding tanks. *Antilloorgia*, *Gorgonia ventalina*, *Plexaurella*, *Acropora palmata*, were suspended in the larger tank on the left to reduce stress. Macroalgae and smaller hard coral chunks were kept in the tank on the right. The filtering system can be seen to the right side of the image.

Metabolic Measurements

The samples, depending on their physical size, were placed in either a 140 mL or 1200 mL clear acrylic, temperature-controlled metabolic chamber in order to measure oxygen fluxes at different light intensities (Figure 3). The peduncle of *Antillogorgia* and *Gorgonia ventalina* specimens, and the exposed axial rod of *Plexaurella* specimens were covered with a small amount plasticine clay to form a base and maintain the specimen in an upright position within the metabolic chambers during measurements. Additionally, any exposed surface on rubble samples that occurred during specimen fragmentation and collection was covered with plasticine clay before being placed in the metabolic chambers. The volume of fresh seawater added to each chamber for each measurement was recorded. Oxygen measurements were taken using a Firesting oxygen optode and O₂ logger program. Oxygen measurements were taken for a total of 72 minutes for each sample. Total irradiance time was broken into nine-minute intervals of sample exposure to 0, 50, 100, 200, 300, 450, 900, and 0 Photosynthetically Active Radiation (PAR) $\mu\text{mol photons/m}^2/\text{s}$. The samples were then photographed and frozen for additional processing. Water within the chambers was stirred using stir bars on stir-plates to ensure equal mixing of oxygen within the water mass during oxygen measurements. The chambers were rinsed with filtered freshwater between measurements and the ocean water was exchanged for each sample. All productivity measurements were completed within seven days of collection.



Figure 3. Chambers and light set ups used for metabolic measurements. Left picture is the 1200 mL chamber used for larger specimens, light shines on these specimens from the side. Right picture is the 140 mL chamber used for smaller, flatter specimens. Light shines on these specimens from above.

Specimen Surface Area calculations

After metabolic measurements were completed, the tissue was removed from the hard coral specimen fragments using a Water Pik™ filled with filtered freshwater. Surface areas for the hard coral and rubble specimens were then determined using the aluminum foil method (Marsh 1970). The images of the macroalgae and soft coral specimens were processed through a photograph homography tool in MATLAB in order to correct for image angle orientation and normalizing image pixel count to surface area ($10,000 \text{ pixels} = 1 \text{ cm}^2$). The outline of the macroalgal and soft coral samples (except for *Plexaurella*) in the corrected images were taken in the Image J program, and the surface areas for each sample were calculated from the measured

pixel area. In order to determine the surface area for *Plexaurella* samples, the radius and length of each branch of the *Plexaurella* in the corrected images were measured in Image J. The surface area of the whole specimen was determined by applying the formula for the surface area of a cylinder for each branch on the specimen. These branch surface areas were then summed together after subtracting the base area from one side of each branch cylinder to account for the branch connection points on the specimen.

Annotated 3-D Reef Site Models

Images were acquired for the 3-D reconstruction and annotation of varying sized tracts of reef in the Florida Keys using a stereovideo camera (Dual GoPro 3+ Black). A snorkeler swam 1-3 m above the reef in a lawnmower pattern while recording 2.7k video at 30 frames per second. Images were extracted at 1-4 frames per second and 3-D reconstructions were generated using Agisoft Photoscan with images from a single camera. Images were paired from the stereo video to provide a metric scale for the 3-D reef reconstruction. The mesh faces on the 3-D reconstruction were mapped back to the original images in which features were visible to apply photo-textures from the original videos onto the 3-D model. Finally, a Convolutional Neural Network designed to annotate images of reef benthos was applied to the 3-D reconstructions to classify the reef surfaces into 15 categories of varying taxonomic resolution with 90% accuracy (annotation method similar to Andrew King et al. 2018). These 15 categories were defined as: Algae (a combination of benthic sections of reef that entail patches of *Dictyota spp.*, *Styopodium spp.*, and *Halimeda spp.*), Pink algae (*Galaxuara spp.*), *Plexaurella* (sea rods), *Antillogorgia*, *Gorgonia ventalina*, *Porites astreoides*, *Siderastrea siderea*, *Orbicella* (a combination of benthic sections of reef that are identified as colonies of *Orbicella annularis* or

Orbicella faveolata), *Acropora cervicornis*, *Acropora palmata*, Rubble, Sand, Other (visually identifiable sections of the reef benthos that are not any of the previous categories), Unclassified (sections of reef benthos that could not be identified due to image quality), and Not Seen (sections of the reef that were not included in the 3-D reef reconstructions due to the angle of filming or swim pattern taken while acquiring the stereo-video transects). The 3-D reef reconstructions and benthic annotations were developed and provided by Dr. Brian M. Hopkinson.

Light Field Model

A light field model was applied to the annotated 3-D reef reconstructions in order to estimate the amount of PAR light that strikes each surface over the course of a day. The model considers direct and diffuse light and calculates the amount of incident light on the 3-D triangular mesh faces of the 3-D reef reconstructions. The irradiance input into the system over the course of the modeled sunlight hours was determined from use of the Simplified Model of Atmospheric Radiative Transfer of Sunshine (SMARTS Windows version 2.9.5i1.3) (Gueymard 2005). The output of the SMARTS model was based off the use of the built in Subtropical Summer reference atmosphere, Maritime aerosol model, a regional and tilted surface albedo of water/calm ocean, a spectral range of 400 nm to 700 nm, for the hours of 6 AM to 7 PM on July 5, 2017, on surfaces with a range of tilt and azimuth angles, at the coordinates of N 25°06'21.6", W 80°18'25.2" (Little Grecian Reef). A diffuse attenuation coefficient for downwelling irradiance (K_d) of 0.1 m^{-1} (rough estimate based on Zepp et al. 2008 and Ong et al. 2018) was applied to the model in order to account for light absorption and scattering by the water column above the reef benthos. Overall, the light field model determines the direct and diffuse

photosynthetic photon flux ($\mu\text{mol Photons}/\text{m}^2/\text{s}$) that strikes each 3-D face at a given sun angle over the course of the modelled daylight hours.

Data Analysis and Application of Bottom-up Model

A total of 205 autotrophic specimen oxygen flux versus light intensity data sets were analyzed in Matlab to determine the Maximum Gross Primary Production (GPP) rates, Respiration rates (R), the light saturation parameter (E_k) values, and a saturating fit of net photosynthesis versus irradiance. GPP was calculated as the NPP measured in the light plus the R measured in the dark phases of the metabolic chamber measurements. Maximum GPP and R rates were normalized to the surface area of each corresponding specimen. The Productivity rates normalized to surface area of each sample of the same taxa were averaged together to produce productivity rates for each measured taxa and for each season (Winter or Summer) that the measurements took place in. The metabolic rates of *Dictyota spp.*, *Styopodium spp.*, and *Halimeda spp* were averaged together to apply to the “Algae” annotated surfaces. The metabolic rates of *Orbicella annularis* and *Orbicella faveolata* were averaged together to apply to the “*Orbicella*” annotated surfaces. The metabolic rates applied to the *Acropora cervicornis* and *Siderastrea siderea* annotated surfaces were an average of the rates of all of the other measured hard coral surfaces (no *Acropora cervicornis* or *Siderastrea siderea* were sampled during any of the field seasons).

The Summer season GPP, R, E_k , and saturating exponential fit of net photosynthesis versus irradiance values for each taxa were applied with the light field model to the annotated 3-D reconstructions of seven reef sites in order calculate the total the GPP rates and Net Primary Productivity (NPP) rates for each site over the course of the light hours of a day. The total

contribution and percent contribution of each taxon to the productivity of each site, as well as the surface area contribution of each taxon to the 3-D site reconstruction from the final model outputs were calculated in Excel. A linear regression was performed between the percent surface area contribution and percent GPP contribution for each taxon at each site. A Pearson product-moment Correlation was run in R using the stats package (R Core Team 2016) in order to analyze the relationship between site specific GPP percentage and producer surface area percentage contributions. The maximum GPP rates, maximum Respiration rates, and E_k values for all samples were checked for normality for each taxon. T-tests were performed on the data in order to develop 95% confidence intervals for the max GPP, max Respiration, and E_k values for each experimentally measured taxon.

RESULTS

Metabolic Measurements

The average maximum gross primary productivity (mGPP) rates ($\mu\text{mol O}_2/\text{cm}^2/\text{s}$) for all taxa, as determined through the P. vs. E experiments, were estimated from a total of 205 samples (figure 4). The taxa were divided into two general groups- one being the group of taxa with symbiotic, photosynthetic dinoflagellates (corals), and the other group being the taxa of macroalgae (algae). The maximum GPP rates normalized to surface area and error bars were derived based on 95% confidence intervals. *Galaxuara* had the highest mGPP rates with mean $7.17\text{e-}04 \mu\text{mol O}_2/\text{cm}^2/\text{s}$, 95% CI [$4.56\text{e-}04$, $9.79\text{e-}04$]. *Plexaurella* (sea rod) and Rubble had the lowest mGPP value with mean $1.05\text{e-}04 \mu\text{mol O}_2/\text{cm}^2/\text{s}$, 95% CI [$9.38\text{e-}05$ $1.16\text{e-}04$] and mean $1.59\text{e-}04 \mu\text{mol O}_2/\text{cm}^2/\text{s}$, 95% CI [$1.32\text{e-}04$, $1.87\text{e-}04$] respectively. All algae group members were not significantly different from each other based on the 95% confidence intervals. For the coral group, *G. ventalina* and *Antilloorgia* were significantly different from each other based on the 95% CI. The rest of the confidence intervals for the coral group taxa overlap except for *Plexaurella*. Rubble and *Plexaurella* mGPP rates were significantly lower than all other measured taxa and were significantly different from each other.

The average light saturation parameter, E_k values ($\mu\text{mol photons}/\text{m}^2/\text{s}$), was estimated from all measured samples (Winter and Summer samples) for each taxon, as determined from the P. vs. E experiments (figure 5). 95% confidence intervals for E_k values were derived for all taxa in order to compare estimated values. *Acropora palmata* had the highest E_k value with mean 247 $\mu\text{mol photons}/\text{m}^2/\text{s}$, 95% CI [33.73, 460.27]. *Stypopodium* had the lowest E_k value with mean

112.79 $\mu\text{mol photons/m}^2/\text{s}$, 95% CI [82.87, 142.72]. All algae group E_k values were similar based on the 95% confidence intervals. In the coral group, all E_k 95% confidence intervals overlap except for *G. ventalina* and *Plexaurella*. The estimated Rubble E_k values were significantly different from all taxa except for *Acropora palmata*, *Plexaurella*, and *Orbicella faveolata*.

The average respiration rates ($\mu\text{mol O}_2/\text{cm}^2/\text{s}$) were estimated from all measured samples (Winter and Summer samples) for each taxon, as determined from the P. vs. E experiments (figure 6). 95% confidence intervals were derived for the respiration rates of all taxa in order to compare estimated values. In general, algae taxa group respiration rates were low and statistically similar to each other. Coral group taxa respiration rates, in general, were higher than the algae group respiration rates, and similar to each other with the exception of *Plexaurella*. The *Plexaurella* respiration rate was significantly lower than the respiration rates of the other coral group taxa. *Plexaurella* and Rubble respiration rates were statistically similar to the lower algae group respiration rates based on the 95% confidence intervals.

Net Primary Production (NPP) P. v E. curves ($\mu\text{mol O}_2/\text{cm}^2/\text{s}$ vs. $\mu\text{mol Photons/m}^2/\text{s}$) were derived from the metabolic measurements at increasing Irradiance levels (illustrated in figure 7). Rubble displayed the most inactive NPP output with increasing irradiance, while the algae taxa displayed the two highest NPP outputs with increasing irradiance. The coral group taxa NPP rates with increasing Irradiance were more similar to each other based on the overlapping data points.

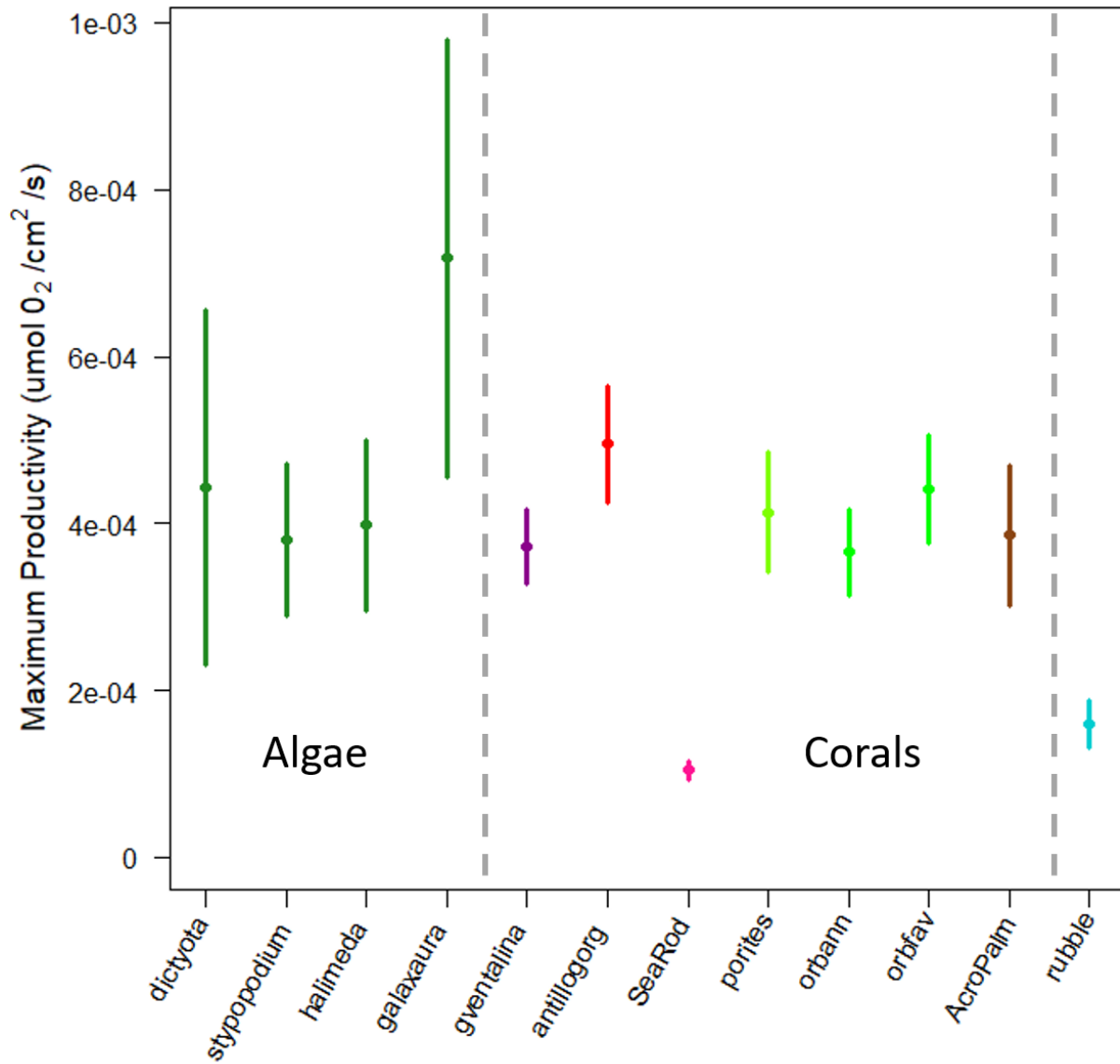


Figure 4. Maximum GPP rates for measured taxa. Coral group representing taxa with symbiotic, photosynthetic dinoflagellates and the algae group representing the macroalgae. Center dots are the mean values of the max GPP rates and the lines represent 95% confidence intervals.

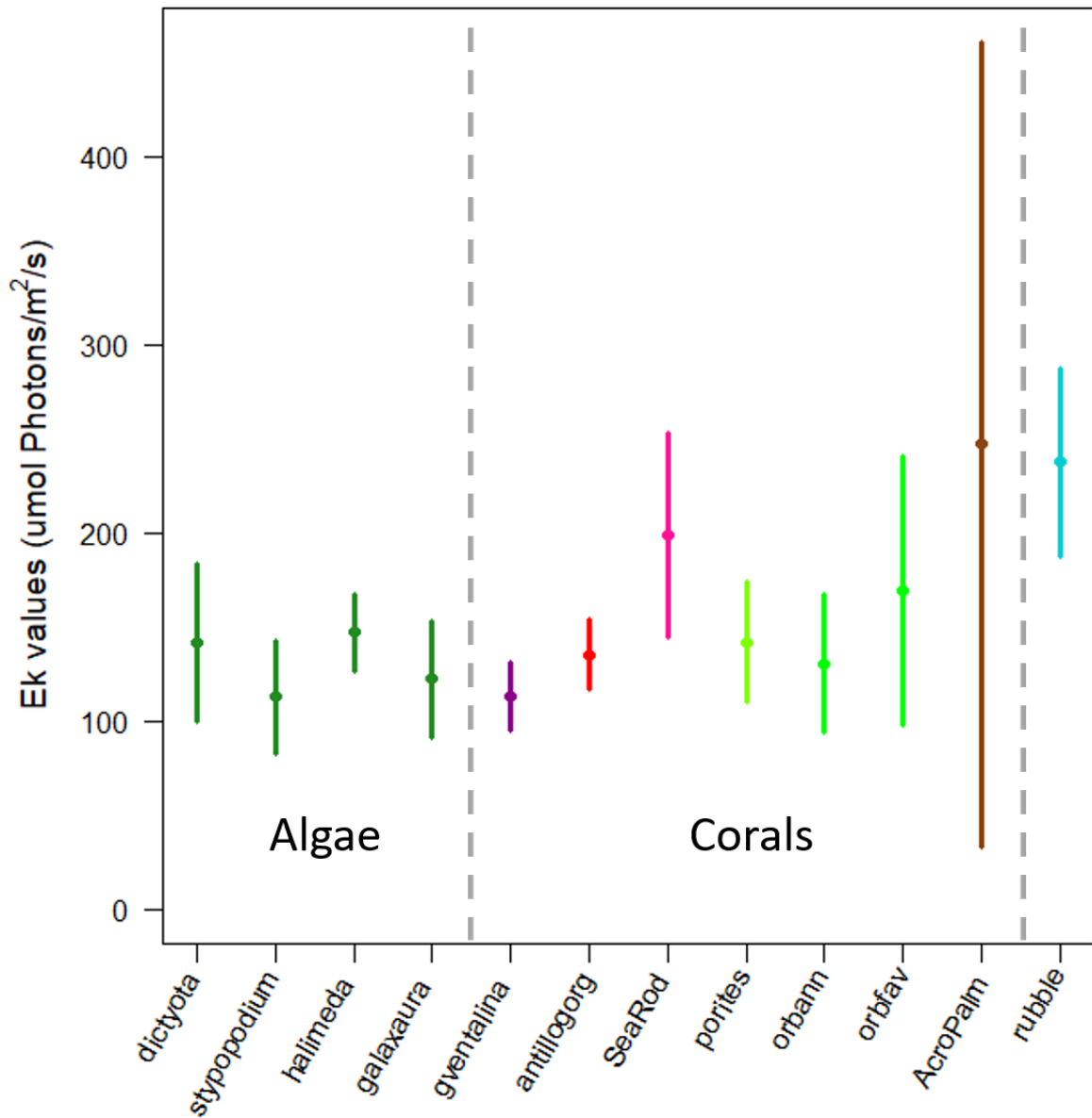


Figure 5. Light saturation parameter (E_k) values for max GPP measurements. Coral group representing taxa with symbiotic, photosynthetic dinoflagellates and the algae group representing the macroalgae. Center dots are the mean values of the max GPP rates and the lines represent 95% confidence intervals.

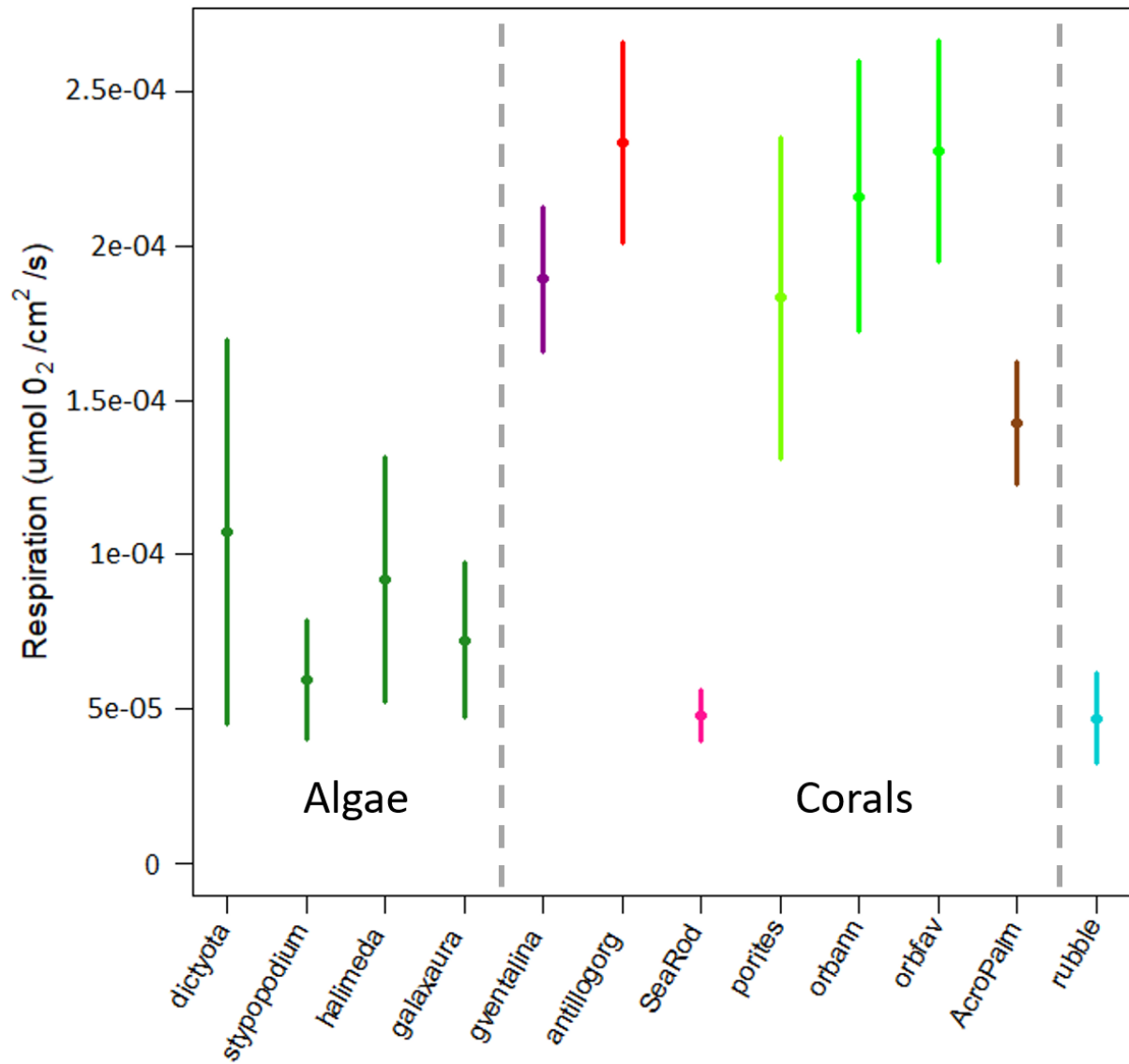


Figure 6. Respiration rates for each measure taxa. Coral group representing taxa with symbiotic, photosynthetic dinoflagellates and the algae group representing the macroalgae. Center dots are the mean values of the max GPP rates and the lines represent 95% confidence intervals.

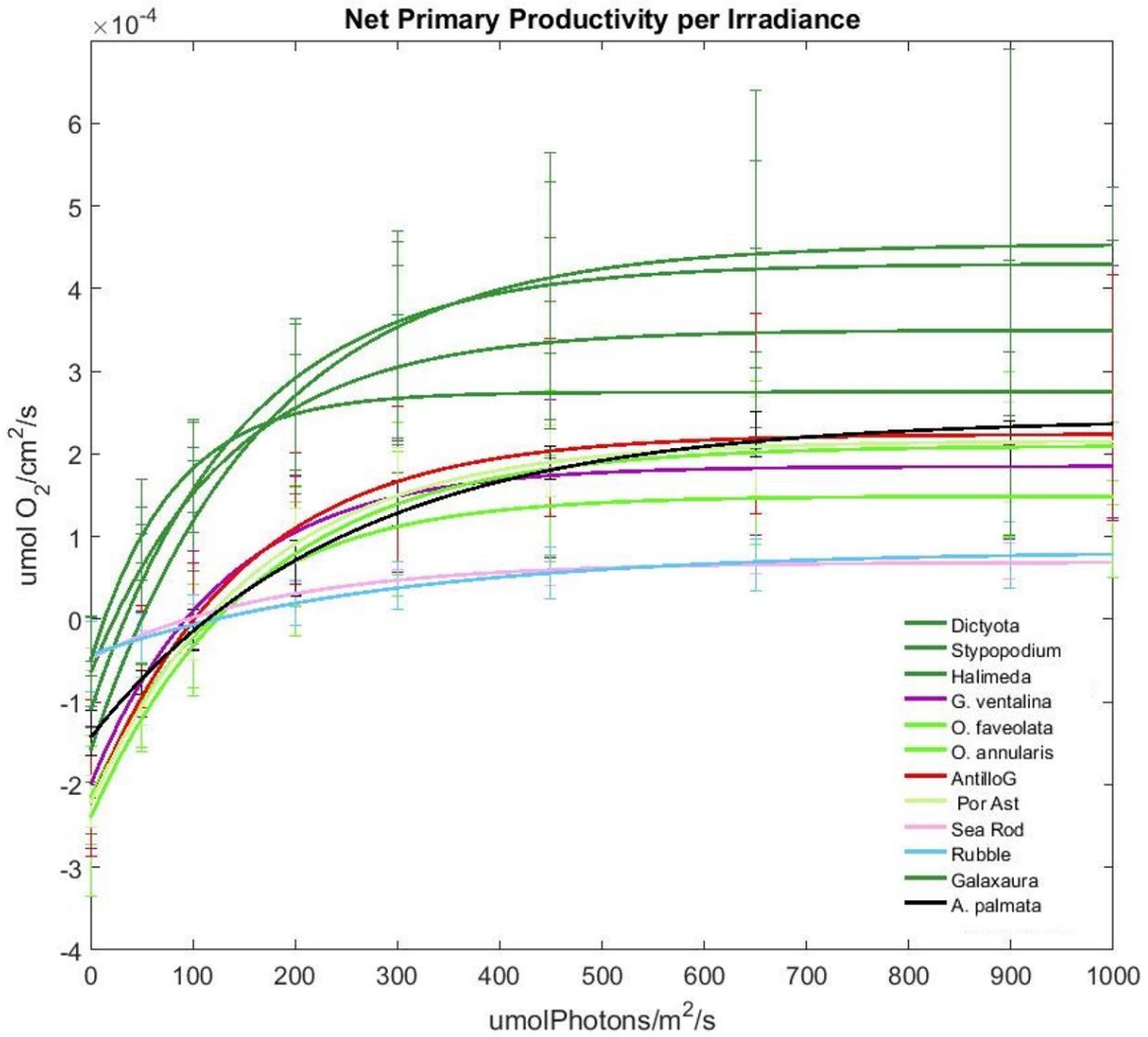


Figure 7. NPP rates for measured taxa for increasing levels of irradiance. Lines represent the fitted trend, with error bars representing the standard deviation of NPP measurements for each taxon at each irradiance that had multiple data points. This figure does not include the complete set off all metabolic measurements taken and is only meant to be illustrative of the trends and values that were applied in the bottom-up model.

3-D Reef Scale Primary Production

3-D benthic reef surface reconstructions were developed for seven reef sites. The 3-D surface area of the reconstructed reef sites ranged from 132.1 m² (site 457) to 2,350 m² (site 215). Figure 8 illustrates the end results of the 3-D reconstruction and benthic annotation process. Percent surface area contributions for all 15 categories of benthic surface were calculated for each site (table 1). Rubble was the most common labelled surface among all 15 categories, contributing between 16.43% to 48.75% of the 3-D benthic surface between the seven reefs sites. Site 457 represents a relatively “pristine” reef site with hard coral *Acropora palmata* constituting 32% of the benthic surface area, while site 215 represents a relatively “degraded” reef site with Rubble constituting 37.54% of the benthic surface area (table 1). Site 457 and site 215 will be used to further compare the final bottom-up model application results. The 3-D reconstructions and annotations for each site are illustrated in figure 9.

The light field model and Summer season metabolic rates (table 2) were applied to the 3-D annotated reef reconstructions in order to generate estimates of GPP and Net Primary Productivity (NPP) rates by surface area (mmol O₂/m²/hr) for each site over the light hours (6am to 7pm) of a single day. GPP rates are lowest in the low light hours (sunset and sunrise) of the day and are highest during midday when incoming irradiance and surface area struck by PAR is maximized for each site (figure 10). Each site is net heterotrophic during the low light hours (6am and 7pm), and net autotrophic for the remaining daylight hours (figure 11). Total GPP and NPP rates per surface area for each site were summed over the course of the modelled day (table 3). Site 622 was found to have the highest GPP rate (234.64 mmol O₂/m²/day) and NPP rate (112.46 mmol O₂/m²/day). The total daily GPP results for each site were estimated to be similar values and ranged from 141.92 mmol O₂/m²/day (site 441) to 234.64 mmol O₂/m²/day (site 622)

(figure 12). However, the total percent GPP contribution of each photosynthetic taxa was partitioned differently among each site (figure 13, table 4). These GPP contribution differences coincide with the estimated producer surface area percentage abundances for each site (figure 14, table 5). The Pearson's product-moment correlation supports that the relationship between producer taxa GPP percent contribution and the producer taxa surface area percent contribution for all sites is not random ($t = 12.375$, $df = 68$, $p\text{-value} < 2.2e-16$, $r = 0.8321758$). A linear regression (figure 15) of producer percent GPP contribution versus percent surface area contribution results in an equation of $y = 0.7979x + 2.0208$, with the producer taxa percent surface area contribution explaining 69.25% of the producer taxa GPP variance ($r^2 = 0.6925$).

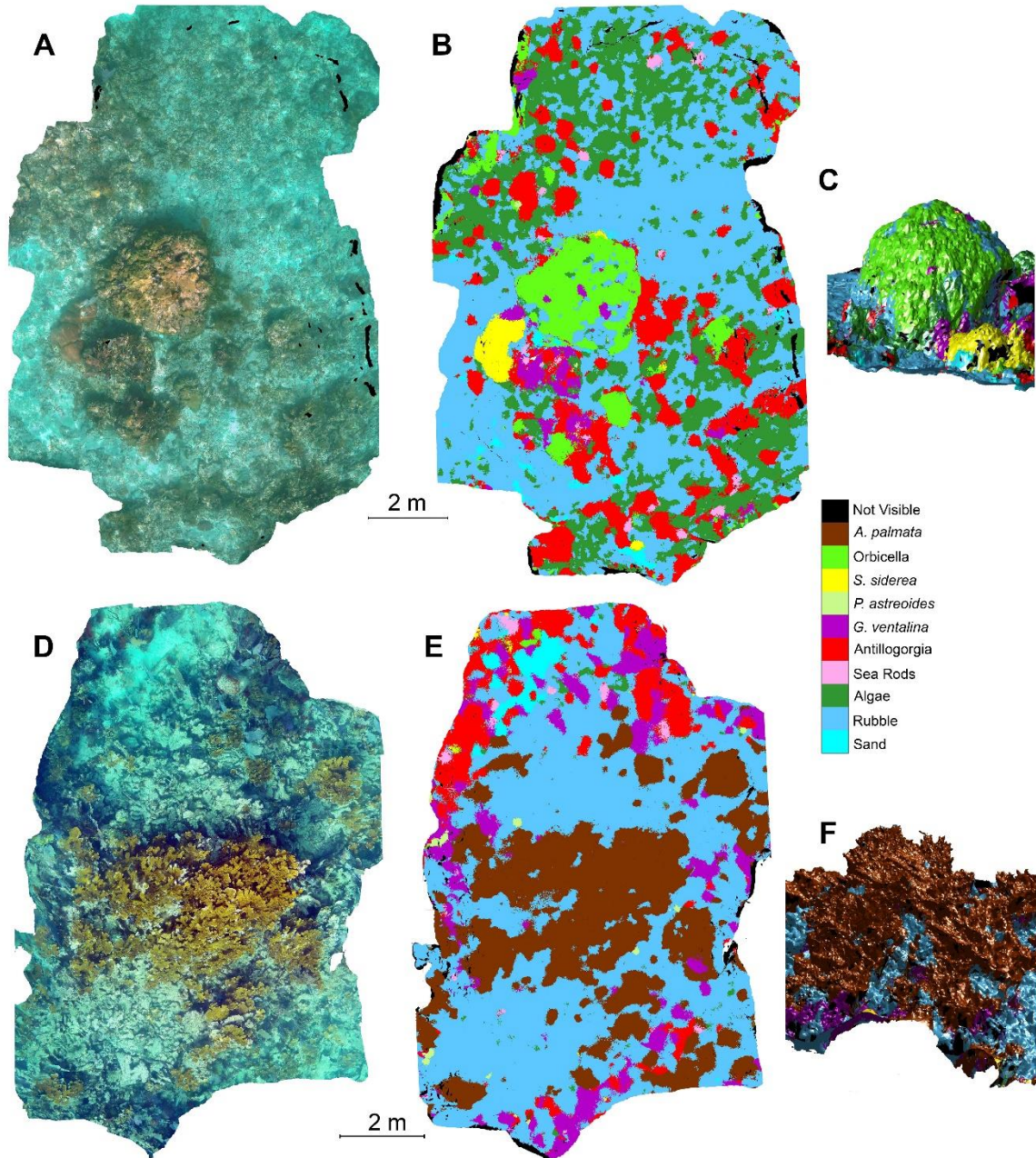


Figure 8. Examples of the 3-D reconstruction and benthic annotation of reef sites. A, B, D and E illustrate a top down view of the 3-D reconstruction. B and E show the annotation of the benthic surfaces. C and F show a portion of the side view of each annotated reef site to demonstrate reconstruction dimensionality.

Table 1. Surface area contribution (percent %) of all benthic classifications on each site.

| | site 215 | site 441 | site 443 | site 453 | site 457 | site 622 | site 623 |
|-----------------------|----------|----------|----------|----------|----------|----------|----------|
| <i>A. cervicornis</i> | 0 | 0.18 | 0.01 | 0.01 | 0 | 0 | 0 |
| <i>A. palmata</i> | 0.22 | 0.05 | 0.12 | 30.95 | 32.00 | 0.19 | 0.22 |
| <i>Orbicella</i> | 1.07 | 6.10 | 9.58 | 0.13 | 0.01 | 0.02 | 0.07 |
| <i>S. siderea</i> | 0.20 | 2.15 | 1.76 | 0.08 | 0.11 | 0.13 | 0.23 |
| <i>P. astreoides</i> | 1.29 | 0.31 | 0.12 | 0.29 | 0.85 | 4.99 | 6.17 |
| <i>G. ventalina</i> | 14.41 | 1.57 | 3.38 | 9.16 | 10.56 | 19.15 | 14.64 |
| <i>Antillogorgia</i> | 15.84 | 11.10 | 17.47 | 7.21 | 8.37 | 26.33 | 24.84 |
| <i>Plexaurella</i> | 5.34 | 1.68 | 0.90 | 0.69 | 0.23 | 1.51 | 1.88 |
| Algae | 0.54 | 15.96 | 22.80 | 0.51 | 1.08 | 17.27 | 18.98 |
| <i>Galaxaura</i> | 12.04 | 0 | 0 | 0 | 0 | 0 | 0 |
| Rubble | 37.54 | 48.75 | 35.01 | 41.25 | 32.70 | 16.43 | 21.56 |
| Sand | 1.93 | 3.34 | 1.09 | 1.14 | 0.56 | 3.73 | 2.12 |
| Unclassified | 0 | 0 | 0 | 0 | 0 | 0 | 0 |
| Other | 4.51 | 0 | 0 | 0 | 0 | 0 | 0 |
| Not Seen | 5.07 | 8.81 | 7.78 | 8.58 | 13.52 | 10.24 | 9.29 |

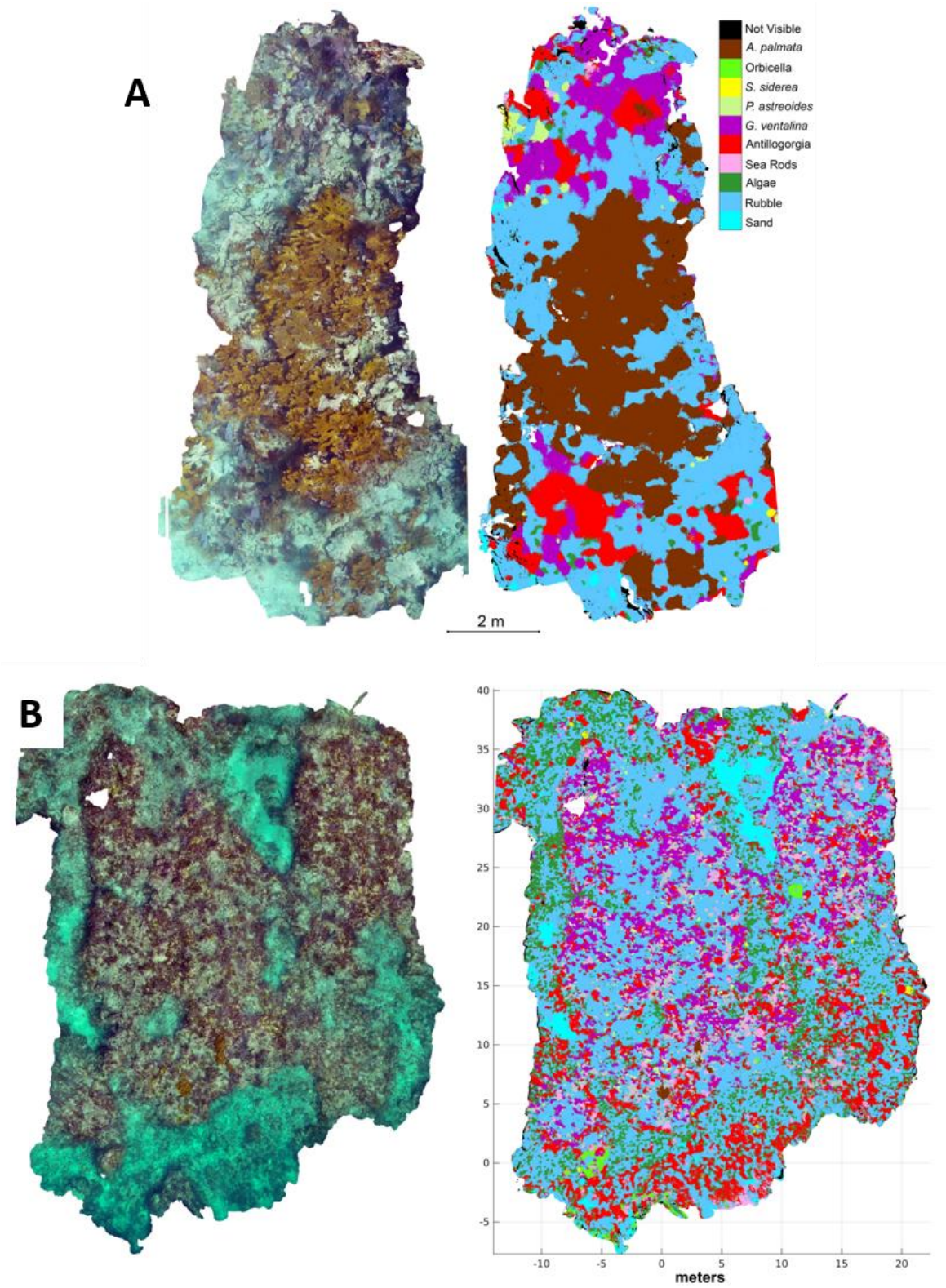


Figure 9. Top down view of 3-D reconstruction and benthic annotation of site 457 (A) and site 215 (B).

Table 2. Maximum Gross Primary Production, Light Saturation constants, and Respirations values for each taxa applied to the 3-D annotated models and Light field model to generate Summer primary production estimates.

| Taxa | max GPP ($\mu\text{mol O}_2/\text{m}^2/\text{s}$) | Ek ($\mu\text{mol Photons}/\text{m}^2/\text{s}$) | Respiration ($\mu\text{mol O}_2/\text{m}^2/\text{s}$) |
|-----------------------|---|--|---|
| <i>A. cervicornis</i> | 4.06 | 1.80E+02 | 2.02 |
| <i>A. palmata</i> | 3.86 | 2.47E+02 | 1.43 |
| <i>Orbicella</i> | 4.08 | 1.67E+02 | 2.28 |
| <i>S. siderea</i> | 4.06 | 1.80E+02 | 2.02 |
| <i>P. astreoides</i> | 4.21 | 1.38E+02 | 2.1 |
| <i>G. ventalina</i> | 3.64 | 1.21E+02 | 1.94 |
| <i>Antillogorgia</i> | 5.12 | 1.43E+02 | 2.5 |
| <i>Plexaurella</i> | 1.08 | 1.63E+02 | 0.47 |
| Algae | 4.45 | 1.32E+02 | 0.96 |
| <i>Galaxaura</i> | 3.86 | 8.40E+01 | 0.53 |
| Rubble | 1.59 | 2.54E+02 | 0.53 |
| Sand | 0 | 1 | 0 |
| Unclassified | 0 | 1 | 0 |
| Other | 0 | 1 | 0 |

Table 3. Total GPP and NPP rates over light hours (6am-7pm) of one day for each site.

| | GPP ($\text{mmol O}_2/\text{m}^2/\text{day}$) | NPP ($\text{mmol O}_2/\text{m}^2/\text{day}$) |
|----------|--|--|
| site 215 | 169.30 | 85.14 |
| site 441 | 141.92 | 76.16 |
| site 443 | 194.61 | 100.70 |
| site 453 | 198.37 | 72.53 |
| site 457 | 200.90 | 78.45 |
| site 622 | 234.64 | 112.46 |
| site 623 | 221.18 | 111.95 |

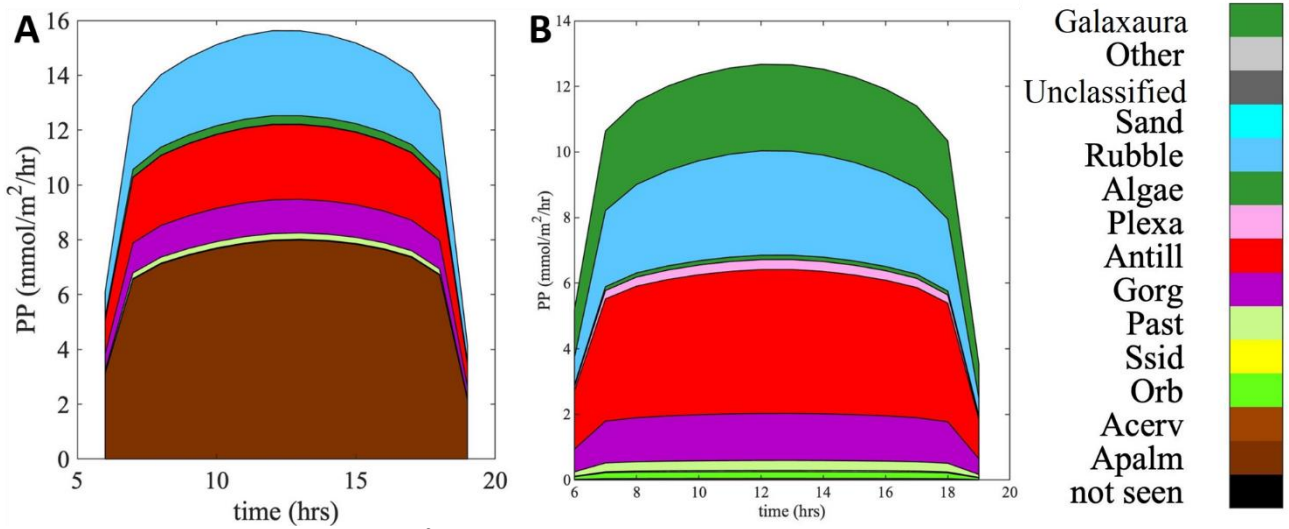


Figure 10. GPP rates ($\text{mmol O}_2/\text{m}^2/\text{hour}$) from 6am to 7pm on reef site 457 (A) and site 215 (B) based on the bottom-up model implementation.

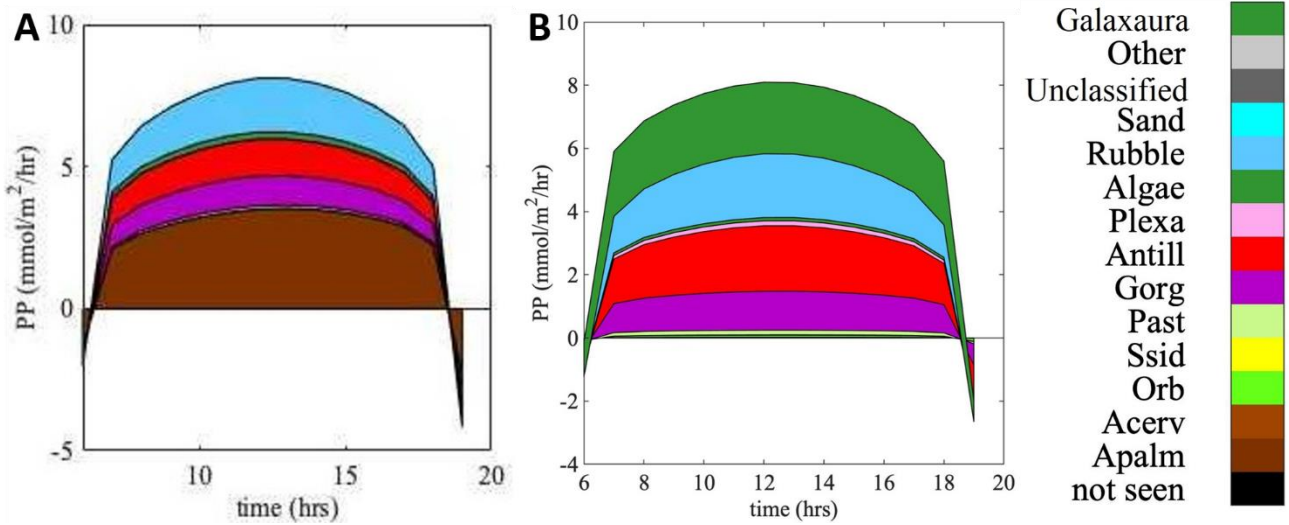


Figure 11. NPP rates ($\text{mmol O}_2/\text{m}^2/\text{hour}$) from 6am to 7pm on reef site 457 (A) and site 215 (B) based on the bottom-up model implementation. Negative PP values represent time when the system is net-heterotrophic.

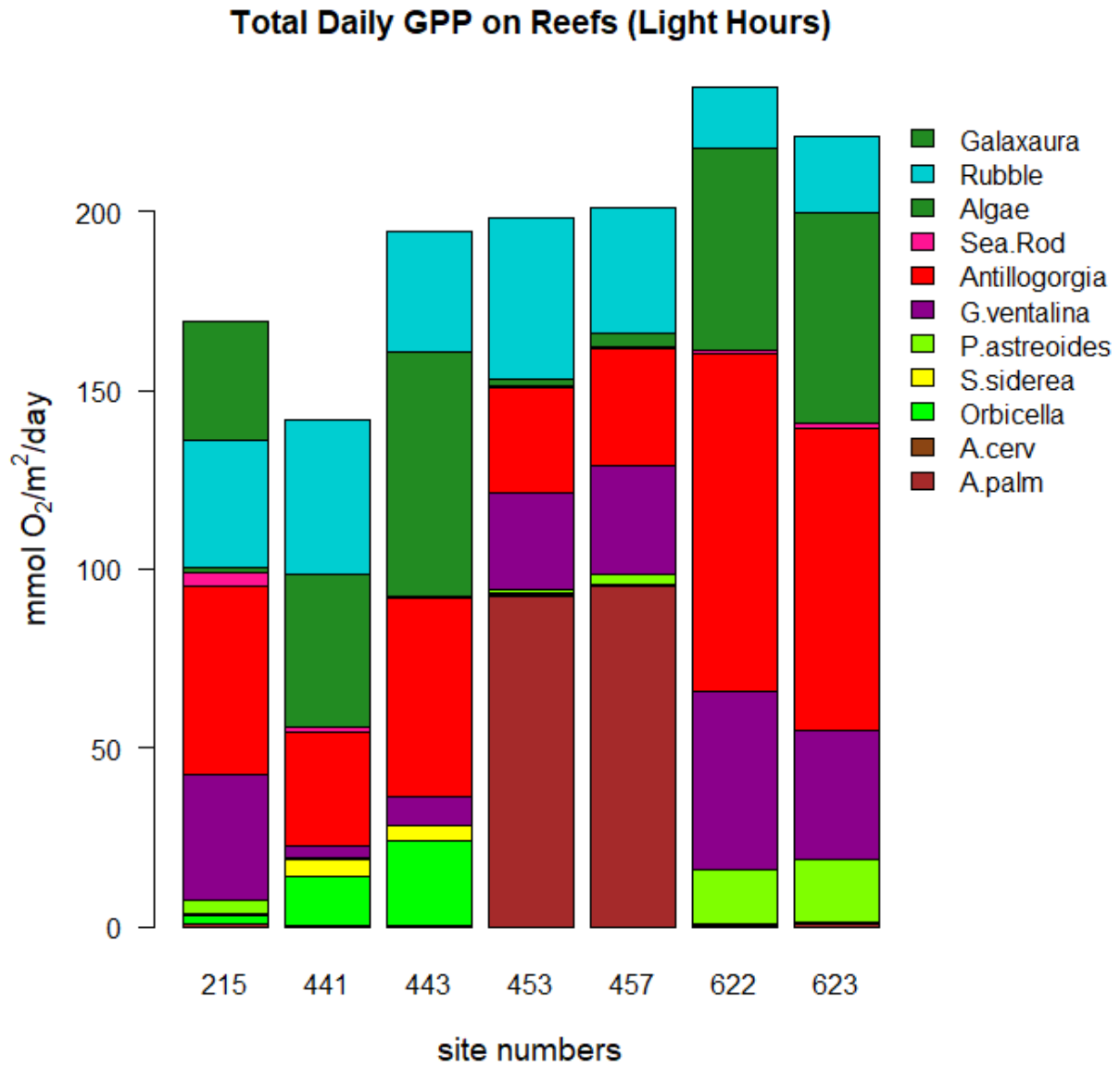


Figure 12. The total Daily GPP and partitioning of production on modeled reef sites during light hours (6am-7pm). PP partitioning is associated with surface area cover for each producer group.

Productive Taxa Contribution to Total Daily GPP on Reefs

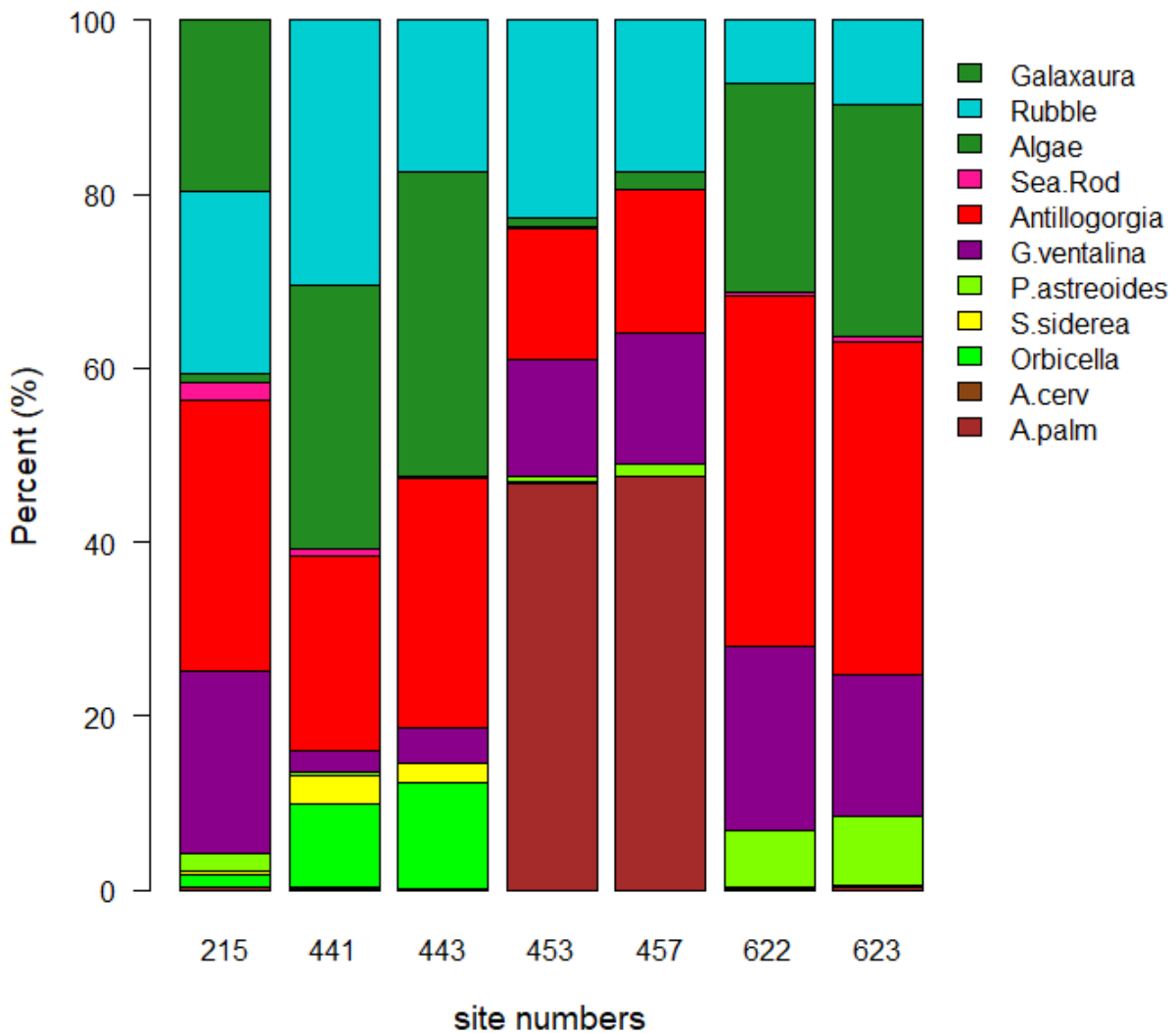


Figure 13. Percent contribution of each photosynthetic taxa to the total daily GPP over light hours (6am-7pm) for each reef site.

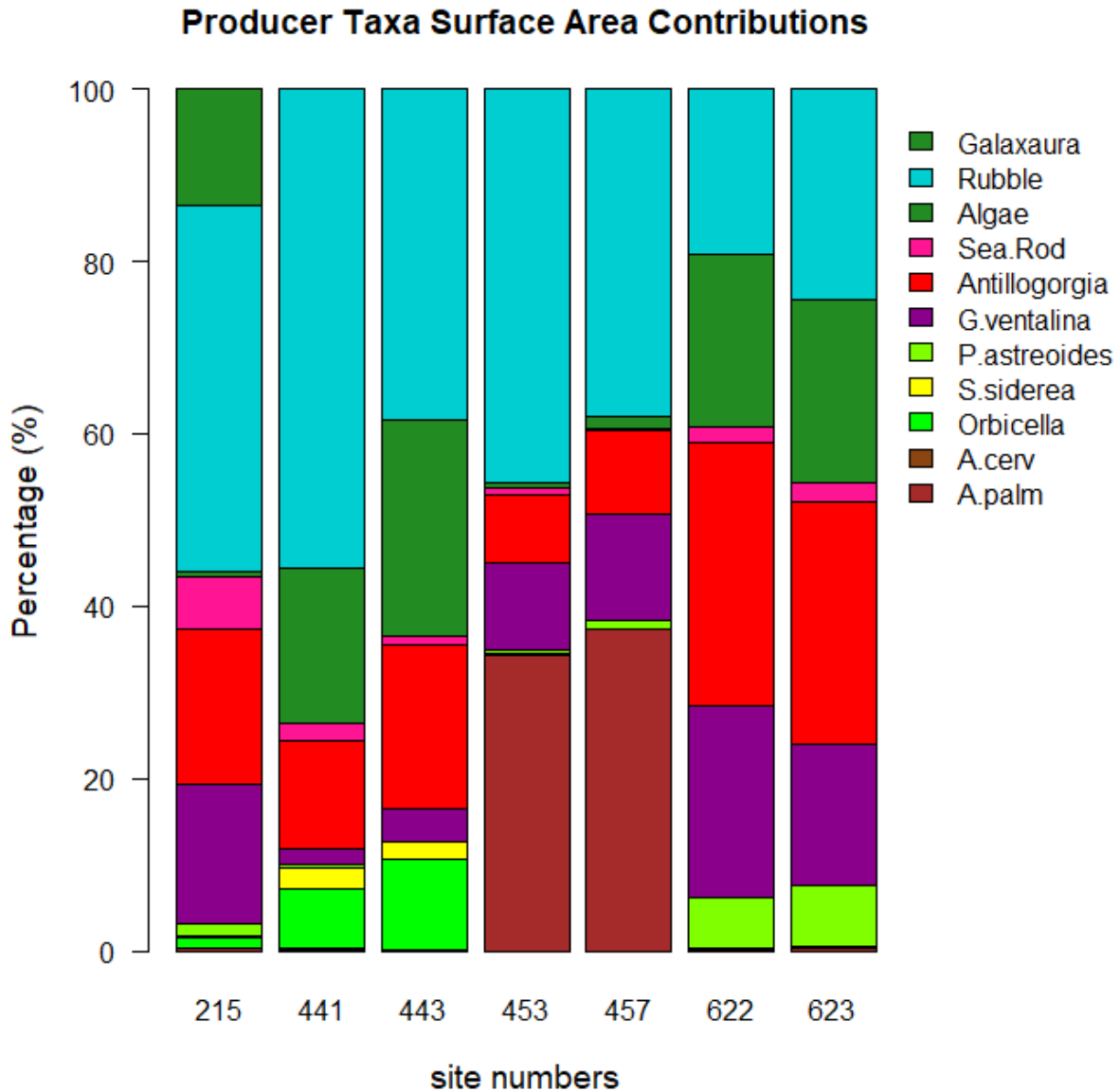


Figure 14. 3-D surface area percent coverage for photosynthetic taxa at each reef site. Rubble comprises a significant portion (16.4% - 48.8%) of coverage on each site. For all taxa, surface area contribution coincides with GPP contribution for each site ($r^2 = 0.6925$).

Table 4. Producer taxa GPP contribution (%) to total light hours GPP per reef site.

| | site 215 | site 441 | site 443 | site 453 | site 457 | site 622 | site 623 |
|-----------------------|----------|----------|----------|----------|----------|----------|----------|
| <i>A. cervicornis</i> | 0 | 0.26 | 0.01 | 0.01 | 0 | 0.0 | 0.00 |
| <i>A. palmata</i> | 0.33 | 0.07 | 0.13 | 46.66 | 47.46 | 0.21 | 0.25 |
| <i>Orbicella</i> | 1.47 | 9.61 | 12.26 | 0.21 | 0.01 | 0.02 | 0.08 |
| <i>S. siderea</i> | 0.27 | 3.22 | 2.10 | 0.14 | 0.17 | 0.15 | 0.27 |
| <i>P. astreoides</i> | 2.20 | 0.49 | 0.15 | 0.50 | 1.40 | 6.45 | 7.92 |
| <i>G. ventalina</i> | 20.90 | 2.31 | 3.97 | 13.56 | 15.02 | 21.11 | 16.21 |
| <i>Antillogorgia</i> | 31.06 | 22.52 | 28.63 | 14.89 | 16.44 | 40.28 | 38.34 |
| <i>Plexaurella</i> | 2.14 | 0.71 | 0.31 | 0.29 | 0.09 | 0.47 | 0.58 |
| Algae | 0.97 | 30.24 | 34.93 | 0.95 | 1.90 | 24.11 | 26.56 |
| <i>Galaxaura</i> | 19.61 | 0 | 0 | 0 | 0 | 0 | 0 |
| Rubble | 21.04 | 30.57 | 17.51 | 22.79 | 17.50 | 7.19 | 9.79 |

Table 5. Producer Taxa only Surface Area contribution (Percent %) for each site.

| | site 215 | site 441 | site 443 | site 453 | site 457 | site 622 | site 623 |
|-----------------------|----------|----------|----------|----------|----------|----------|----------|
| <i>A. cervicornis</i> | 0 | 0.20 | 0.01 | 0.01 | 0.00 | 0.00 | 0.00 |
| <i>A. palmata</i> | 0.25 | 0.05 | 0.13 | 34.28 | 37.25 | 0.22 | 0.25 |
| <i>Orbicella</i> | 1.20 | 6.95 | 10.51 | 0.14 | 0.01 | 0.02 | 0.08 |
| <i>S. siderea</i> | 0.23 | 2.45 | 1.93 | 0.09 | 0.13 | 0.15 | 0.26 |
| <i>P. astreoides</i> | 1.46 | 0.35 | 0.13 | 0.32 | 0.99 | 5.80 | 6.97 |
| <i>G. ventalina</i> | 16.28 | 1.79 | 3.71 | 10.15 | 12.29 | 22.26 | 16.53 |
| <i>Antillogorgia</i> | 17.90 | 12.64 | 19.17 | 7.98 | 9.74 | 30.61 | 28.03 |
| <i>Plexaurella</i> | 6.04 | 1.91 | 0.98 | 0.77 | 0.27 | 1.76 | 2.12 |
| Algae | 0.61 | 18.16 | 25.01 | 0.56 | 1.25 | 20.08 | 21.42 |
| <i>Galaxaura</i> | 13.60 | 0 | 0 | 0 | 0 | 0 | 0 |
| Rubble | 42.42 | 55.50 | 38.42 | 45.69 | 38.06 | 19.09 | 24.34 |

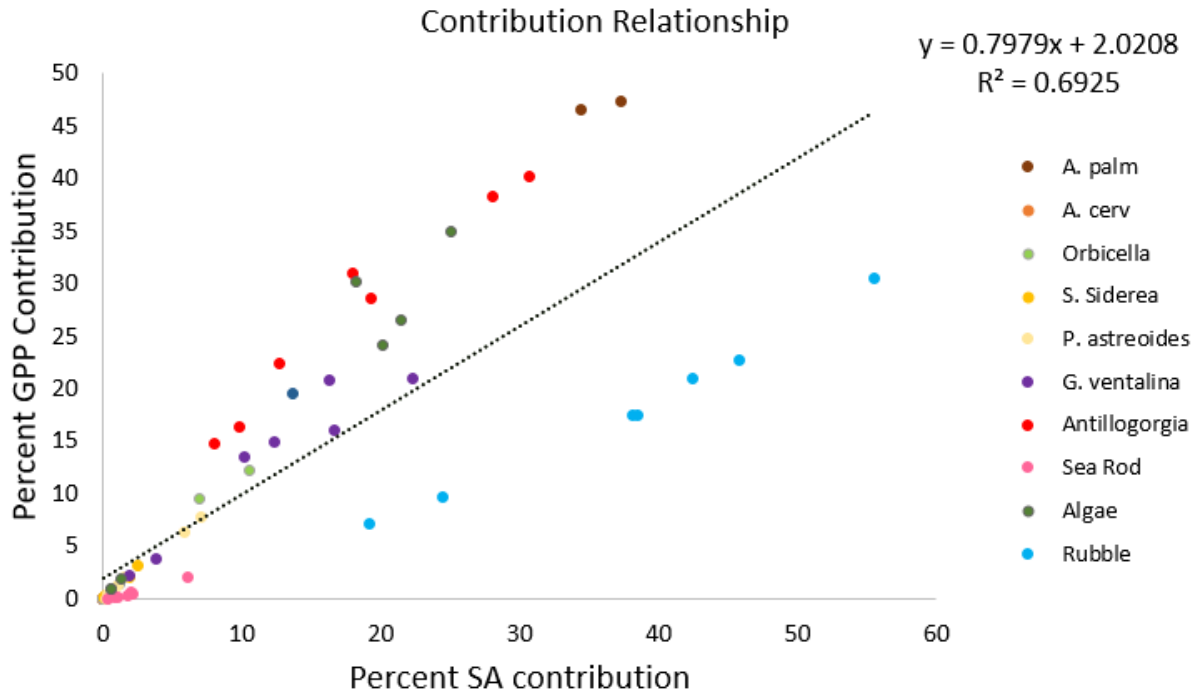


Figure 15. Linear regression relating percent surface area contribution for each photosynthetic taxa to percent contribution to light hours GPP based on a total of 70 data points. Taxa surface area explains 69.25% of the taxa GPP variance ($r^2 = .6925$).

DISCUSSION

Bottom-Up Model Productivity Estimate Comparisons

Recently, Eddy Covariance (EC) measurements of reef metabolism have been taken within the Grecian Rocks Sanctuary Protection Area of the Florida Keys National Marine Sanctuary (Long et al. 2013). The EC study area was similar to the sites modelled in this bottom-up approach (but not the same exact site locations) and allows for a comparison of EC measured *in-situ* “top-down” whole ecosystem productivity rates with the gross primary productivity estimates from the bottom-up method. The reef crest GPP rate per day determined through EC measurements was $\sim 950 \text{ mmol O}_2/\text{m}^2/\text{day}$, whereas the GPP for reef crest areas estimated from the bottom-up approach ranged from 142 to $235 \text{ mmol O}_2/\text{m}^2/\text{day}$ (figure 16). The GPP estimates of the bottom-up approach are of the same order of magnitude as the EC GPP measurements, but are only about one-third of the *in-situ* measured reef crest GPP. The bottom-up method GPP rates per day were more similar to the EC measured reef slope areas ($\sim 193 \text{ mmol O}_2/\text{m}^2/\text{day}$) than the EC measured reef crest areas. The sites modelled in the bottom-up approach are considered to be reef crest areas, but the modelled sites do have benthic percent cover partitioning similar to the reef slope areas measured by the EC methods (47% rubble and sand benthic planar surface cover).

There are a few factors that may be contributing to the bottom-up model underpredicting system productivity. The 3-D reconstructions of the site areas cannot fully resolve all the producer biomass in the area. In particular, the 3-D reconstructions underestimate the 3-D surface area of any producer that may be moving due to water flow action while the stereo-video

transects were being taken. This specifically affects the soft coral taxa, for example. This lower 3-D surface area estimate will result in an underestimate of the total productivity contributed by the soft corals in the bottom-up model. Further, the handling of organisms during collection from reef sites and during the metabolic measurements may negatively affect the photosynthetic processes of each sample. The sample organism handling may also lend itself to the disparity seen between the light intensities at which the EC measured ecosystem and individually measured bottom-up taxa PvE curves become saturated. The *in-situ* EC measurements of the coral reef site do not show light saturation until 1750 $\mu\text{mol photons/m}^2/\text{s}$, whereas the PvE curves applied in the bottom-up model begin to saturate around 200 $\mu\text{mol photons/m}^2/\text{s}$. On one hand, the noticeably higher *in-situ* coral reef ecosystem E_k values may not reflect accurate individual organism E_k . Due to the 3-D habitat complexity of a coral reef ecosystem, not all of the light entering a reef area at any given moment will be shining directly on each individual primary producer surfaces at all times. This may be an explanation of why the whole ecosystem light saturation values are so high compared to the individual light saturation values applied within the bottom-up model. However, lower PvE light saturation values are a common trend found among PvE curves estimated through metabolic chamber methods (e.g. Chalker et al. 1983). The PvE curves applied in the bottom-up model can saturate just from the input of diffuse light striking each surface. *In-situ*, the un-stressed organisms may individually exhibit a higher light saturation parameter. Therefore the primary producers captured by the EC method measurements may have the potential for higher productivity rates than the stressed organisms measured in the metabolic chambers applied within the bottom-up model.

There have been previous attempts to estimate reef ecosystem productivity through bottom-up approaches. Two recent examples of scaling up taxon-specific rates to estimate

ecosystem primary production include a study conducted in a coral reef lagoon near Puerto Morelos, Mexico (Naumann et al. 2013) and a study based in a Caribbean coral reef off the coast of Columbia (Eidens et al. 2014). In each of these studies, the productivity of each producer functional group was scaled up by its photosynthetic surface area in the system, similar to the bottom-up approach described in our methods. The 3-D surface areas of the benthic producers in the two studies were estimated from a 2-D to 3-D area conversion factor based on 2-D photo-transects of the benthic environment. The coral reef lagoon bottom-up model reported GPP estimates of ~488 mmol O₂/lagoon area/day, with more than half of the daily GPP contribution coming from the seagrasses present in the lagoon system. The Columbian coral reef bottom-up model produced GPP estimates of 250 – 305 mmol O₂/m² seafloor/day. These bottom-up reef productivity estimates are comparable to the 142 - 235 mmol O₂/m²/day range estimated in the approach discussed in this study. The bottom-up model estimates for the coral reef lagoon and Colombian coral reef however do not consider the irradiance striking the photosynthetic surfaces over the course of a day. The bottom-up approach in this study does attempt to assess the response of metabolic rates on reef producers to *in-situ* production driving factors, through the application of the daylight irradiance model onto the 3-D reef reconstructions. Therefore, the metabolic rates and total daily productivity estimates produced from this bottom-up approach may more accurately reflect productivity rates *in-situ* compared to previous bottom-up approach studies.

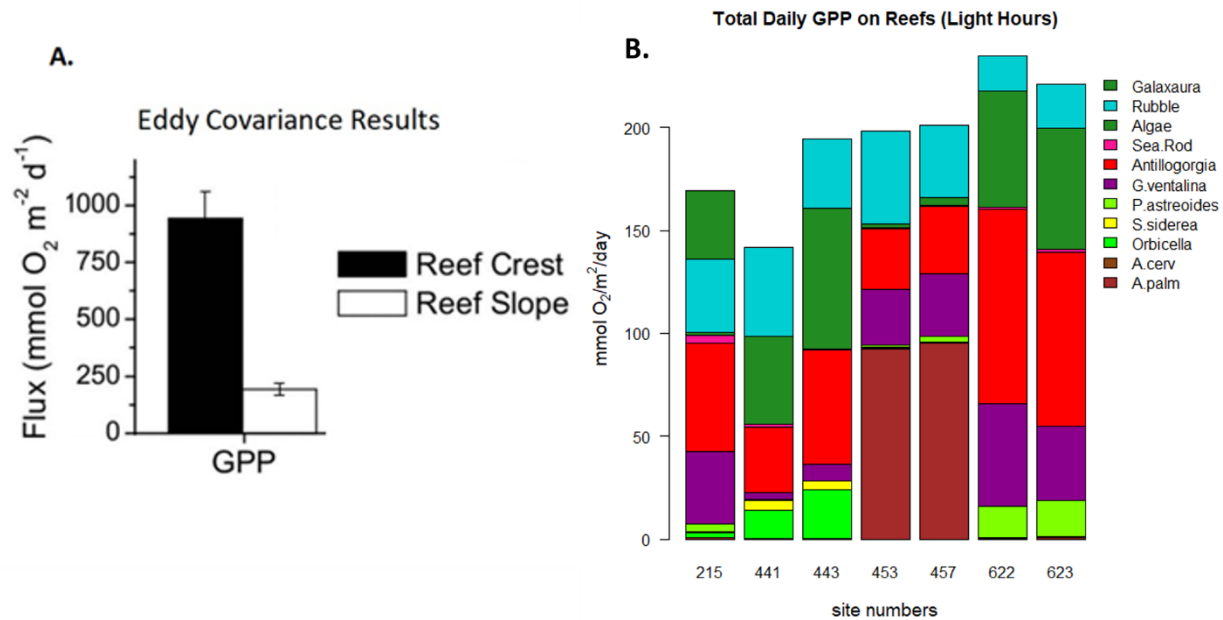


Figure 16. Eddy Covariance measurements of reef GPP over 24 hours (adapted from Long et al. 2013). B) GPP estimates from bottom up model approach over 14 hours (light hours). Sites used for the bottom up model are considered closer to “reef slope” areas than “reef crest” areas based on location.

Bottom-Up Model Implications

With the caveat of possibly underestimating total ecosystem productivity, this bottom-up approach to estimating reef ecosystem productivity allows for a determination of how productivity is partitioned among benthic community members. Further, it was found that the contribution of each of these community members to each site productivity is correlated with the taxon’s 3-D surface area contribution. This relationship offers insight into how productivity will be affected with changes in benthic community member surface area percent cover. These changes in benthic community surface area contributions can result from events such as hurricane damage, coral bleaching events with no recovery, and the on-going processes of coral reef phase shifts seen especially in the Caribbean (Sweatman et al. 2011). These processes are actively occurring in reef areas around the world and on relatively short timescales. For example,

during the field data collection for this study, Hurricane Irma affected the benthic reef community in a way that was noticeable within the bottom-up model. Before the 2017 hurricane event, no *Galaxaura* algae was noticed in any of the site reconstructions. After the hurricane event, *Galaxaura* algae became a significant contributor to reef site 3D surface area, and Gross and Net Primary Productivity (Site 215, table 4 and table 5). On top of the storm damage that decreased the amount of living hard coral in reef areas, this single hurricane event quickly shifted the benthic community in a way that can have long-lasting impacts on the coral reef area ecology. When herbivores are present, production from macroalgae more directly supports higher trophic organisms and increasing macroalgae cover will cause a shift in the nutrient cycling dynamics of the reef system (Hughes et al. 1987). Without herbivore grazing, macroalgae can produce large amounts of labile organic matter that may induce growth of microbial coral pathogens, and feed into the phase shifts seen in reef ecosystems around the world (Smith et al. 2006).

With the loss of hard coral from reef sites, the community is losing the source of carbon from exuded coral mucus. This is a loss of carbon assimilated into the reef area microbial loop as well as a loss of a mechanism for the tight carbon recycling found in the reef system (Muscatine and Porter 1977). Increases in soft coral cover such as *Gorgonia ventalina* and *Antilloporia* can functionally replace the mucus exuded by hard corals (Wild et al. 2004). However, with the loss of living hard coral, the reefs are losing the main structure and habitat building organisms of the ecosystem. This causes losses in habitat complexity and can negatively affect ecosystem services provided by coral reefs. As living hard coral cover is lost, the space is replaced by rubble and the cryptic algae that live on the rubble. Looking at the trends in producer taxa surface area contribution to producer taxa GPP contribution (figure 15), rubble cover in general produces less

GPP per day than the hard coral taxa when the group percent surface area contributions are similar. Increases in rubble cover that coincide with hard coral loss will overall decrease total GPP and NPP found in the reef ecosystems. This can have significant implications on the nutrient recycling and the ability for the ecosystem to provide habitat for higher trophic level organisms.

Bottom-Up Model Conclusions

In conclusion, this bottom-up approach to estimate taxon-specific primary production rates on coral reefs can model the dynamics of production for a defined reef area over the light hours of a day. Further the application of this model allows for an estimate of how primary production is partitioned among benthic community producers on a reef. Finally, it was found that producer taxa GPP and 3-D surface area percent contribution are correlated, with the surface area percent contribution explaining a large amount of taxa GPP variation.

Coral reefs are in a dangerous, critical state today and are constantly impacted through anthropogenic forces, weather events, ocean warming, and ocean acidification. This bottom-up approach to estimating coral reef productivity can help researchers predict how past and future changes in species abundance and diversity on reefs will affect system level productivity, and in turn how these changes in productivity can affect coral reef system ecology.

REFERENCES

- Al-Najjar M. A.A., D. de Beer, M. Kühl, L. Polerecky. 2012. Light utilization efficiency in photosynthetic microbial mats. *Environ Microbiol* 14: 982–992.
- Burke, L., K. Reytar, M. Spalding, and A. Perry. 2011. Reefs at Risk Revisited. World Resources Institute.
- Carpenter, R. C. 1986. Partitioning herbivory and its effects on coral-reef algal communities. *Ecol. Monogr.* 56: 345-363.
- Chalker B.E., W.C. Dunlap, J.K. Oliver. 1983. Bathymetric adaptation of reef-building corals at Davies Reef, Great Barrier reef, Australia. II. Light saturation curves for photosynthesis and respiration. *J Exp Mar Biol Ecol* 73: 37–56.
- Davies, P. S. 1984. The role of zooxanthellae in the nutritional energy requirements of *Pocillopora eydouxi*. *Coral Reefs* 2:181-186.
- Eidens, C., E. Bayraktarov, T. Hauffe, V. Pizarro, T. Wilke, C. Wild. 2014. Benthic primary production in an upwelling-induced coral reef, Colombian Caribbean. *PeerJ* 2:e554; DOI 10.7717/peerj.554.
- Gardner, T. A., I. M. Cote', J. A. Gill, A. Grant, A.R. Watkinson. 2003. Long-term region-wide declines in Caribbean corals. *Science* 301(5635):958-60.
- Graham, N. A. J., K. L. Nash, J. T. Kool. 2011. Coral reef recovery dynamics in a changing world. *Coral Reefs*. DOI 10.1007/s00338-010-0717-z.
- Gueymard C. 2005. Interdisciplinary applications of a versatile spectral solar irradiance model: a review. *Energy* 30, 1551-1576.
- Hughes, T. P., D. C. Reed, M. Boyle. 1987. Herbivory on coral reefs: community structure following mass mortalities of sea urchins. *Jour. of Exp. Mar. Biol. and Ecol.* 113 (1): 39-59.
- Hughes, T. P. 1994. Catastrophes, phase shifts, and large-scale degradation of a Caribbean coral reef. *Science*, New Series, Vol. 265, No. 5178, pp. 1547-1551.
- King, A., S. M. Bhandarkar, B. M. Hopkinson; The IEEE Conference on Computer Vision and Pattern Recognition (CVPR) Workshops, 2018, pp. 1394-1402.

- Long, M. H., P. Berg, D. De Beer, and J.C. Zieman. 2013. In Situ Coral Reef Oxygen Metabolism: An Eddy Correlation Study. *PLoS One* 8 e58581.
- Marsh, J. A. 1970. Primary productivity of reef-building calcareous red algae. *Ecology* 51: 255-263.
- Muscantine, L., J. W. Porter. 1977. Reef corals-mutualistic symbioses adapted to nutrient-poor environments. *Bioscience* 27: 454-460.
- Naumann, M. S., C. Jantzen, A. F. Haas, R. Iglesias-Prieto, C. Wild. 2013. Benthic primary production budget of a Caribbean reef lagoon (Puerto Morelos, Mexico). *PLoS One* 8 e82923.
- Odum, H.T., and E. P. Odum. 1955. Trophic Structure and productivity of a windward coral reef community on Eniwetok Atoll. *Ecol. Monogr.* 25: 291-320.
- Ong, R. H., A. J.C. King, M. J. Caley, B. J. Mullins. 2018. Prediction of solar irradiance using ray-tracing techniques for coral macroand micro-habitats. *Mar. Environ. Research* 141: 75-87.
- Smith, J. E., M. Shaw, R. A. Edwards, D. Obura, O. Pantos, E. Sala, S. A. Sandin, S. Smriga, M. Hatay, and F. L. Rohwer. 2006. Indirect effects of algae on coral: algae-mediated, microbe-induced coral mortality. *Ecology Letters*, 9: 835–845.
- Sweatman, H., S. Delean, C. Syms. 2011. Assessing loss of coral cover on Australia's Great Barrier reef over two decades with implications for long-term trends. *Coral Reefs*, 30: 521- 531.
- Wild, C., M. Huettel, A. Klueter, S. G. Kremb, M. Y. M. Rasheed, and B. B. Jorgensen. 2004. Coral mucus functions as an energy carrier and particle trap in the reef ecosystem. *Nature* 428: 66-70.
- Zepp, R. G., G. C. Shank, E. Stabenau, K. W. Patterson, M. Cyterski. 2008. Spatial and temporal variability of solar ultraviolet exposure of coral assemblages in the Florida Keys: Importance of colored dissolved organic matter. *Limnol. Oceanogr.* 53(5), 1909–1922.